Biochimica et Biophysica Acta 1787 (2009) 1468–1478

Contents lists available at ScienceDirect

Biochimica et Biophysica Acta

journal homepage: www.elsevier.com/locate/bbabio

Photochemical and photoelectrochemical quenching of chlorophyll fluorescence in photosystem II

Wim Vredenberg [a,*,1], Milan Durchan [b], Ondřej Prášil [c,1]

[a] Department of Plant Physiology, Wageningen University and Research, Wageningen, The Netherlands
[b] Faculty of Biology and Inst. of Physical Biology, University of South Bohemia, Ceske Budejovice, Czech Republic
[c] Laboratory of Photosynthesis, Inst. of Microbiology, Academy of Sciences Czech Republic, Trebon, Czech Republic

ARTICLE INFO

Article history:
Received 20 April 2009
Received in revised form 16 June 2009
Accepted 22 June 2009
Available online 1 July 2009

Keywords:
Chlorophyll a fluorescence
Photosystem II
Heterogeneity
Photochemical quenching
Photoelectrochemical quenching
Kinetic model

ABSTRACT

This paper deals with kinetics and properties of variable fluorescence in leaves and thylakoids upon excitation with low intensity multi-turnover actinic light pulses corresponding with an excitation rate of about 10 Hz. These show a relatively small and amply documented rise in the sub-s time range towards the plateau level F^{pl} followed by a delayed and S-shaped rise towards a steady state level F_m which is between three and four fold the initial dark fluorescence level F_o. Properties of this retarded slow rise are i) rate of dark recovery is $(1–6\ s)^{-1}$, ii) suppression by low concentration of protonophores, iii) responsiveness to complementary single turnover flash excitation with transient amplitude towards a level F_m which is between five and six fold the initial dark fluorescence level F_o and iv) in harmony with and quantitatively interpretable in terms of a release of photoelectrochemical quenching controlled by the trans-thylakoid proton pump powered by the light-driven Q cycle. Data show evidence for a sizeable fluorescence increase upon release of (photo) electrochemical quenching, defined as qPE. Release of qPE occurs independent of photochemical quenching defined here as qPP even under conditions at which qPP = 1. The term photochemical quenching, hitherto symbolized by qP, will require a new definition, because it incorporates in its present form a sizeable photoelectrochemical component. The same is likely to be true for definition and use of qN as an indicator of non photochemical quenching.

1. Introduction

The machinery of photosynthetic light reactions in plants, algae and cyanobacteria is embedded in protein complexes that are oriented in the closed and partially folded membrane system (thylakoid) in the chloroplast. The transverse and lateral orientation and organization of this apparatus in the membrane serve several purposes. (i) The planar separation of two photochemical systems PS I and PS II, laterally connected by cytochrome b_6f complex (cytbf complex) that interacts with plastoquinone pool, allows the uphill electron transfer from water on the donor side of PS II to an intermediate at the acceptor side of PS I. (ii) The trans-membrane orientation of the reaction centers (RCs) of both photosystems in the thylakoid guarantees that exciton trapping, and subsequent charge separation, results in an electrogenic event associated with the generation of a trans-membrane electric potential. Its associated electromotive force acts as a driving force for the generation of electrochemical gradients of ions, in particular protons. (iii) The anchoring and proper orientation of active proton pumps, such as the RCs, the cytbf complex and the ATP synthase which allow the system to function properly [1].

Emission of chlorophyll a (Chl) fluorescence, in brief notation in this paper written as fluorescence, originates for the major part from PS II antenna chlorophylls. It competes with photochemical energy trapping (conversion) in RCs resulting in fluorescence quenching when trapping in the RC is effective [2]. The complementary relation between fluorescence and photochemical yield has made fluorescence monitoring a sensitive non-invasive tool for probing the ongoing electron transport in PS II [3]. Several models have been presented with the goal of quantitatively relating changes in fluorescence yield to the photochemical yield of electron transport to and from PS II [4–15]. The light-dependent fluorescence yield in chloroplasts and intact leaves is variable between a lowest, intrinsic level F_o (the "O" level) at full photochemical quenching under dark-adapted conditions and a maximal level F_m (the "P" level) at saturating light intensities at which all quenching is released. Variable fluorescence is defined as $F_v = F_m - F_o$. The primary quinone electron acceptor of PS II, Q_A, has since long been known as the major and principal quencher; the quenching is released upon its photoreduction [16]. F_m is commonly associated with full reduction of Q_A and with a trapping-incompetent closed RC. Other additional

* Corresponding author. Laboratory of Plant Physiology, Wageningen University and Research, Droevendaalsesteeg 1, 6708 PB Wageningen, The Netherlands. Tel.: +31 317 482147; fax: +31 317 484740.
E-mail address: wim.vredenberg@wur.nl (W. Vredenberg).

[1] Dedicated to the memory of Ivan Setlik, our highly esteemed and beloved senior-colleague in photosynthesis research, who died on 13 April 2009 in Trebon at the age of 80.

0005-2728/$ – see front matter © 2009 Elsevier B.V. All rights reserved.
doi:10.1016/j.bbabio.2009.06.008

Glossary and abbreviations

β	fraction of Q_B-nonreducing RCs with $\beta=\beta_0$ for S_0 fraction in dark-adapted samples
DCMU	3(3,4-dichlorophenyl)-1,1-dimethylurea
DSQ	donor side quenching
FCCP	carbonyl cyanide p-trifluorometoxyphenylhydrazone
$F(t)$	fluorescence emission at time t
$F_m^{S(M)TF}$	fluorescence emission level of system with 100% closed PSUs after S(M)TF excitation in dark-adapted state
F_o	fluorescence emission level of system with 100% open PSUs in dark-adapted state
F^{pl}	$(=\beta^*nF_v^{STF})$ is the 'plateau' level of the relative variable fluorescence associated with release of photochemical quenching in dark-adapted samples upon actinic illumination with low intensity light
$F^{PE}(t)$	fluorescence emission at time t, relative to F_o, associated with release of photoelectrochemical quenching at full and invariable photochemical quenching ($q^{PP}=1$)
$F^{PP}(t)t$	fluorescence emission at time t, relative to F_o, associated with release of photochemical quenching at full and invariable photoelectrochemical quenching ($q^{PE}=1$)
FIA	fluorescence induction algorithm
k_1 (k_{dsq})	rate constant of donor side quenching release
k_{-1}	rate constant of radical pair recombination
k_{AB}	rate constant of Q_A^- oxidation
k_{2AB}	rate constant of oxidation of $[PheQ_A]^{2-}$ in Q_B-nonreducing RCs
k_{dsq}	see k_1
k_L	excitation rate of photosystem in light pulse
k_{-PE}	rate constant of the dark reversion of release of photoelectrochemical quenching and related to trans-thylakoid proton leak (conductance)
k_{qbf}	rate constant associated with light-driven accumulation and reduction of Q_B-nonreducing RCs
$nF_v(t)$	normalized variable fluorescence at time t $\frac{F(t)-F_o}{F_o}$
$nF_v^{S(M)TF}$	normalized variable fluorescence $\frac{F_m^{S(M)TF}-F_o}{F_o}$ upon S(T)MF excitation $nF_v^{MTF}\sim 2^*nF_v^{STF}$
nF_v^{PE}	normalized variable fluorescence associated with full release of photoelectrochemical quenching from $q^{PE}=1$ to $q^{PE}=0$ at full and invariable photochemical quenching ($q^{PP}=1$)
nF_v^{PP}	normalized variable fluorescence associated with full release of photochemical quenching from $q^{PP}=1$ to $q^{PP}=0$ at full and invariable photoelectrochemical quenching ($q^{PE}=1$); $nF_v^{PP}=nF^{STF}$
$rFv(t)$	relative variable fluorescence $\frac{F(t)-F_o}{F_m^{S(M)TF}-F_o}$ at time t in single- (S) and multi- (M) turnover excitation
$rF_v^{PE}(t)$	relative variable fluorescence $\frac{F^{PE}(t)-1}{nF_v^{PE}}$ associated with release of photoelectrochemical quenching at time t
q	fraction of RCs with Q_A^-
q^{PP}	fraction of RCs with 100% photochemical quenching (qPP); index or degree of photochemical quenching with $0\le qPP\le 1$
q^{PE}	fraction of RCs with 100% photoelectrochemical quenching (qPE); index or degree of photoelectrochemical quenching with $0\le qPE\le 1$; can be estimated from the relative area above the $rF_v^{PE}(t)$ $(=1-qPE(t))$ curve at time t: $q^{PE}(t)=\frac{\int_0^t qPE(t)dt}{\int_0^\infty qPE(t)dt}$
qP	photochemical quenching attributed to the difference between F_m and F_o in a sub-s multi-turnover saturating light pulse as commonly used in pulse amplitude modulated (PAM) fluorescence technique
qPP	primary photochemical quenching responsible for light-driven decrease in fluorescence emission under conditions at which the electrochemical potential of ions, in particular protons of which movement is coupled to light-driven electron transport, is invariable
qPE	photoelectrochemical quenching attributed to a decrease in fluorescence emission in response to a change in the electrochemical potential of protons under conditions at which primary photochemical quenching is invariable
MTF	multi-turnover flash (light pulse)
OEC	oxygen evolving complex
ODE	ordinary linear differential equation
PAM	pulse amplitude modulation; dedicated fluorescence detection technology
Ph(e)	pheophytin, primary electron acceptor of PSII
PSII	photosystem II
Q_A	primary quinone electron acceptor of PSII
Q_B	secondary quinone electron acceptor of PSII
RC	reaction center of PS
STF	single turnover flash (excitation)
TTF	twin turnover flash
Y_Z	tyrosine-161 on D1 protein acting as secondary electron donor of PSII

quenchers have been proposed [5,12,17–25] to account for the seeming paradox that the normalized variable fluorescence in a 300 ms multi-turnover pulse (nF_v^{MTF}) is about twice that in a single turnover flash (nF_v^{STF}) [20,26–31]. The fast time-resolved fluorescence induction curve $F(t)$ in a multi-turnover light pulse (MTF excitation), usually of 1 s duration or less, has become known as the so-called OJDIP curve, where "O" is the minimal fluorescence, J is an intermediary maximum, D is the dip that follows, I is another intermediate plateau or inflection and P is the peak at the final maximal fluorescence F_m [32]. The OJD, JDI and IP parts of the curve cover the 0–2.5, 0.3–20 and 20–300 ms time range, respectively and can be identified as distinguishable phases of the OJDIP induction curve. Till now there is debate about the driving force and origin of the distinguished phases, in particular of the JDI- and IP-phase (see for a recent review [33].

The normalized variable fluorescence nF_v $(=F_m/F_o-1)$ in dark-adapted isolated chloroplasts, upon a saturating single (STF) and a twin (TTF) turnover excitation, has been found to be in the range between 1.7 and 2.3, with as an average $nF_v^{TTF}\sim 1.3\ nF_v^{STF}$. The dark recovery of these STF- and TTF-induced fluorescence show a F(ast) (0.01–10 ms) and a S(low) phase extending into the 100 s time range. The S-phase is attributed to the (slow) reoxidation of the reduced Q_A (Q_A^-) in the fraction with Q_B-nonreducing RCs [30,34]. This fraction has been argued [23,35] to be identical with the fraction in which the oxygen evolving complex (OEC) is in the uncharged S_0 state (S_0 fraction). The F-phase of the decay after STF excitation is composed of a major and a minor exponential component. The major component which is invariable in a STF and TTF excitation occurs with an average decay constant k_{AB} $(=1/\tau_1\sim 1/[0.25\ ms]\sim 4\ ms^{-1})$. It is associated with reoxidation of Q_A^- in the RC fraction with Q_B reducing RCs. The minor component, which is substantially higher in the TTF response, decays with a rate constant $k_{2AB}=1/\tau_2\sim 1/[2\ ms]\sim 0.5\ ms^{-1}$ and is attributed to reoxidation of the double-reduced acceptor pair $[PheQ_A]^{2-}$ in Q_B-nonreducing RCs. TTF (double) excitation causes double reduction of acceptor pair in Q_B-nonreducing RCs. Vredenberg et al. [34] have proposed that these RCs are predominantly, if not exclusively, present in the S_0 fraction of dark-adapted thylakoids.

Fluorescence induction responses upon saturating single turnover excitation at various repetition rates have given evidence for a photochemical role and hitherto unrecognized properties of Q_B-nonreducing RCs in PS II electron transport [30,34,36]. The repetitive excitation data have shown that these centers are able to reduce Q_B after a second hit. This is in contrast to what commonly has been assumed about a photochemical inactivity of Q_B-nonreducing RCs in PS II electron transport [37–39]. The fact that reduced Q_B-nonreducing RCs (with Q_A^-) are electron trapping-competent, giving rise to a dark reversible variable fluorescence, suggest that the double-reduced acceptor pair $[PheQ_A]^{2-}$ in these RCs can reduce Q_B. It follows that the term 'Q_B-nonreducing RCs' in fact only refers to OPEN centers of this type. A better nomenclature therefore would be 'Q_B-nonreducing open RCs'. Here we have used the 'traditional' definition and nomenclature of Q_B-nonreducing RCs that has been followed till now in the literature.

This paper focuses upon characteristics and amply documented kinetics of the variable fluorescence measured at very low intensities of actinic light corresponding with an excitation rate of about 10 Hz. These show a relatively small monotonous OJ-rise towards a plateau level $F^{pl}\sim(1.2–1.6)\ F_o$ [32] followed by a delayed S-shaped JI(P)-rise towards a steady state level $F_m^{MTFF}\sim(3–3.8)\ F_o$. Properties of the slow rise are i) rate of dark recovery is $(1–6\ s)^{-1}$, ii) suppression by low concentration of protonophores, iii) responsiveness to complementary STF excitation with transient amplitude $F_m^{MTF+STF}\sim 5F_o$ and iv) in harmony with and interpretable in terms of a release of photoelectrochemical quenching controlled by the trans-thylakoid proton pump powered by the cytbf-driven Q cycle. Evidence is given that release of photoelectrochemical quenching qPE gives rise to a variable fluorescence comparable to, but independent of that associated with release of primary photochemical quenching qPP.

2. Materials and methods

Experiments were done with intact leaves and chloroplasts isolated from pea (*Pisum sativum*). Plant growth, chloroplast isolations and suspending medium were as described elsewhere [30,40]. Room temperature chlorophyll fluorescence yields were measured in dark-adapted chloroplast preparations (1–2 μg/ml) with the Dual-Modulation Kinetic Fluorometer (Photon Systems Instruments, Brno, Czech Republic), as described in detail elsewhere [22,41]. The set-up was routinely used in a mode in which the fluorescence yield during and after N ($1\le N\le 60$) 35 μs single turnover excitations (STFs) in a flash train variable in frequency from 0.3 to 12.5 Hz was probed by weak 3.5 μs measuring flashes, fired at progressing dark intervals in the time domain between 50 μs and 18 s with, on a log time scale 5–10, equidistant excitations per decade. In two particular experiments (see Figs. 2 and 4) the actinic excitation by a 0.33 Hz train of 1 (Fig. 2) or 4 STFs (one STF each 3 s) was supplemented with a multi-turnover light pulse of 5 s duration and very low intensity (<80 μM photons $m^{-2}\ s^{-1}$). The responses are plotted, either on a logarithmic or linear time scale, as the fluorescence signal $F(t)$, relative to the dark fluorescence yield F_o. F_o is the dark fluorescence from antennas with all RCs open, i.e. with the primary quinone acceptor Q_A fully oxidized. STFs were found to be saturating as concluded from the constancy of the relative fluorescence signal F_m/F_o upon 50% decrease in flash intensity, or alternatively in chloroplast density. Further details about the use of this equipment can be found elsewhere [41, and see also http://www.psi.cz)].

Simulation of experimental fluorescence responses $F^{exp}(t)$ were done with application of the fluorescence induction algorithm (FIA) which has been described in detail elsewhere [31,42]. The fit parameters (rate constants, heterogeneity fraction, etc) of the simulation curve $F^{FIA}(t)$ were estimated after application of a dedicated software routine in Mathcad (Mathcad13) which calculates the parameter values (vector) for which a least mean square function $\left[\sum_{n=1}^{NN}\left\{F^{exp}(t_n)-F^{FIA}(t_n)\right\}^2\right]^{1/2}$ is minimal, where NN is the number of data points (in most experiments $40\le NN\le 120$). Exponential decomposition and quadratic least square fitting of the fluorescence decay were done (see also [30,43]) with standard routines provided by appropriate software (MathCad 13, MathSoft Inc. Cambridge, Mass.).

3. Results

Fig. 1 shows the chlorophyll *a* fluorescence response $F(t)/F_o$ in pea chloroplasts upon a 12.5 Hz train of, in this case, 60 single turnover flashes (STF), plotted on a logarithmic time scale. The results are similar to those reported and analyzed earlier [30]. The first flash (STF_1) fired at $t\sim 0$ causes a quenching release (increase in fluorescence) with amplitude relative to F_o equal to nF_v^{STF} ($=F_m^{STF1}-1$) ~ 2.8.

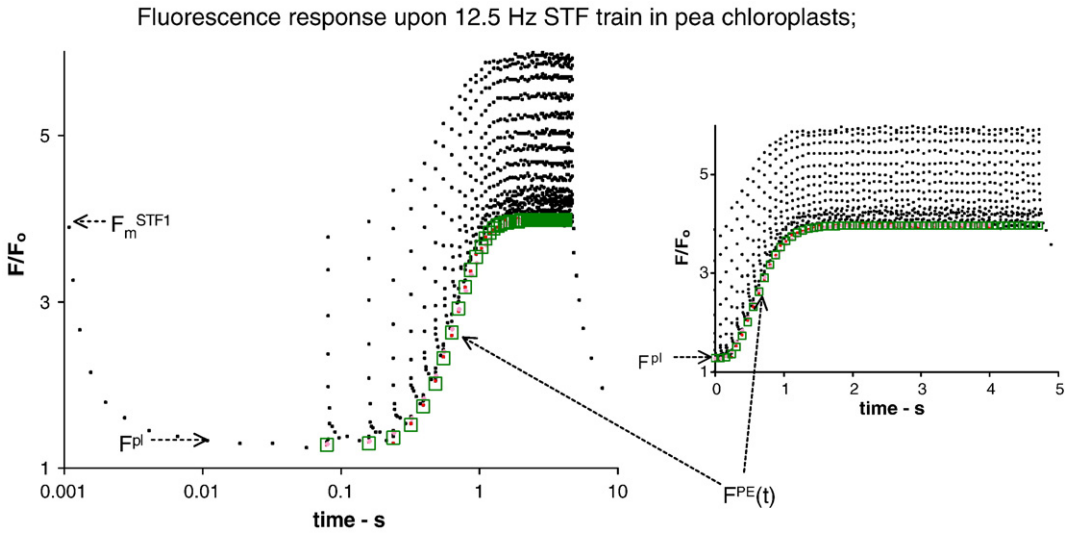

Fig. 1. *Left hand panel* Chlorophyll *a* fluorescence response $F(t)/F_o$ in pea chloroplasts upon a 12.5 Hz train of 60 single turnover flashes (STF) on a logarithmic time scale. The curve connecting the green-colored squares is the log time course of the quasi-steady state fluorescence level at the onset of STFs in the train. These data points coincide with those calculated with the simulation function $F^{PE}(t)$ (Eq. (1)). Parameter values (Eq. (2)) β, nF_v, N, k_{qbf} and $k_{\_\ PE}$ were 0.1, 2.7, 5 and (in s^{-1}) 8 and 0.3, respectively. F^{pl} ($=\beta.\ nF_v$) is the quasi-steady state level in the 10–80 ms time range after STF_1. The experimental data are similar to those reported and analyzed earlier (Vredenberg et al., (2006). *Right hand panel* Same response and curve, plotted on a linear time scale.

It decays within a few ms towards a quasi-steady state level F^{pl} in the 10–80 ms time range. The induction pattern in the subsequent STFs of the train shows a monotonic increase in this quasi-steady state level and in the maximal fluorescence level F_m towards, in this case $F(t)/F_o$ values of ~4 and ~6, respectively. The S-shaped rise in the fluorescence level at the onset of subsequent flashes in the STF train, i.e. the curve obtained after connecting the data points at the lower boundary of the STF-induced oscillating fluorescence response, is shown on a linear time scale in the right hand part of Fig. 1. This lower boundary curve is the one that would have been monitored with a low frequency pass filter in the range between 50 and 100 Hz upon STF illumination with excitation rate 12.5 s^{-1} (12.5 Hz). It should show resemblance (see Fig. 2) to the one measured upon illumination with a low intensity 4 s MTF pulse corresponding with $k_L = 12.5\ s^{-1}$ ($=0.0125\ ms^{-1}$). This boundary curve with its typical sigmoid pattern can be fitted with the function $F(t)/F_o = F^{PE}(t)$. This function can be simulated, in analogy with the simulation of the photoelectrochemical J(D)I phase of the OJDIP fluorescence response in high intensity MTF excitation [42], with the following equation:

$$F^{PE}(t) = 1 + nF_v^{STF}\left[\beta + rFv^{PE}(t)\right] = F^{pl} + nF_v^{STF}[1 - qPE(t)] \qquad (1)$$

in which nF_v^{STF} ($\sim nF_v^{PE}$) is the normalized variable fluorescence upon STF excitation, β is the relative size of the S_0-fraction of Q_B-nonreducing open RCs, $rFv^{PE}(t)$ ($=1-qPE(t)$) is the relative variable fluorescence associated with the release of photoelectrochemical quenching. F^{pl} ($=\beta * nF_v^{STF}$) [44] is the 'plateau' level of the relative variable fluorescence associated with the release of photochemical quenching in a dark-adapted sample upon actinic illumination with low intensity light. We define qPE as the index ($1 \geq qPE \geq 0$) of photoelectrochemical quenching, in analogy with the terminology of qE-, qI- and qI-components of non photochemical quenching [45].

$$qPE(t) = e^{-k_{qbf}\cdot t}\sum_{m=0}^{N}\frac{k_{qbf}{}^{m}}{m!}\frac{k_{qbf}}{k_{qbf}+k_{-PE}}. \qquad (2, (A.3))$$

The derivation of the $qPE(t)$-relation (Eq. (2)) is given in Appendix A.1. The $F^{PE}(t)$ simulation function (Eq. (1)) quantifies the fluorescence response in dependence of rate constants k_{qbf} and k_{-PE} associated with trans-thylakoid proton pumping and -leak, respectively, and of N, which can be thought to be related to effect and number of proton buffering groups in the hydrophilic phases adjacent to the stromal side of the thylakoid [42]. The fit parameters of the simulation curve $F^{PE}(t)$ (open green squares) are given in the legend of Fig. 1. The simulation curve $F^{PE}(t)$ fits well with the curve connecting the experimental data points at the lower boundary of the STF-induced oscillating fluorescence profile.

Fig. 2 shows, for the same preparation as of Fig. 1, the $F(t)/F_o$ response at a simultaneous onset of a 30 μs STF (STF_1) and a low intensity 5 s actinic MTF pulse with excitation rate $k_L \sim 10\ s^{-1}$ in the absence (upper solid curve) and presence (lower dashed curve) of 0.5 μM carbonyl cyanide p-trifluorometoxyphenylhydrazone (FCCP) which acts as a protonic uncoupler of trans-membrane proton movements and has been shown to affect rate and extent of the light-driven accumulation of Q_B-nonreducing RCs associated with release of photoelectrochemical quenching [30,31,34]. Onset of STF_1 and actinic pulse at $t=0$ were with a minimal delay of a few μs. The response pattern upon weak actinic illumination is qualitatively similar to the one upon a 12.5 Hz STF train shown in Fig. 1 in the 0 to 5 s time range. The main difference is a comparatively shorter delay time and a slower rise upon excitation with an MTF pulse. The difference comes into expression in the parameters of the simulation function $F^{PE}(t)$ with a major difference in the N-value in the qPE(t)-expression (Eq. (2)) which is 5 (see legend Fig. 1) and 2 (*ibid.* Fig. 2) for STF and MTF excitation with rate constants (k_{qbf}) of 8 and 3 s^{-1}, respectively. The difference is likely to be caused by the overlap and phase shifts of the subsequent turnovers after onset of the MTF pulse, which is absent in a STF train of discrete frequency. The lower (dashed) curve gives the same light-induced $F(t)/F_o$ response after the addition and in the presence of 0.5 μM FCCP. It is clear that the protonophore does not affect amplitude and dark decay of the STF_1-induced change in fluorescence. In contrast, the rate and amplitude of the fluorescence increase caused by the weak actinic light are

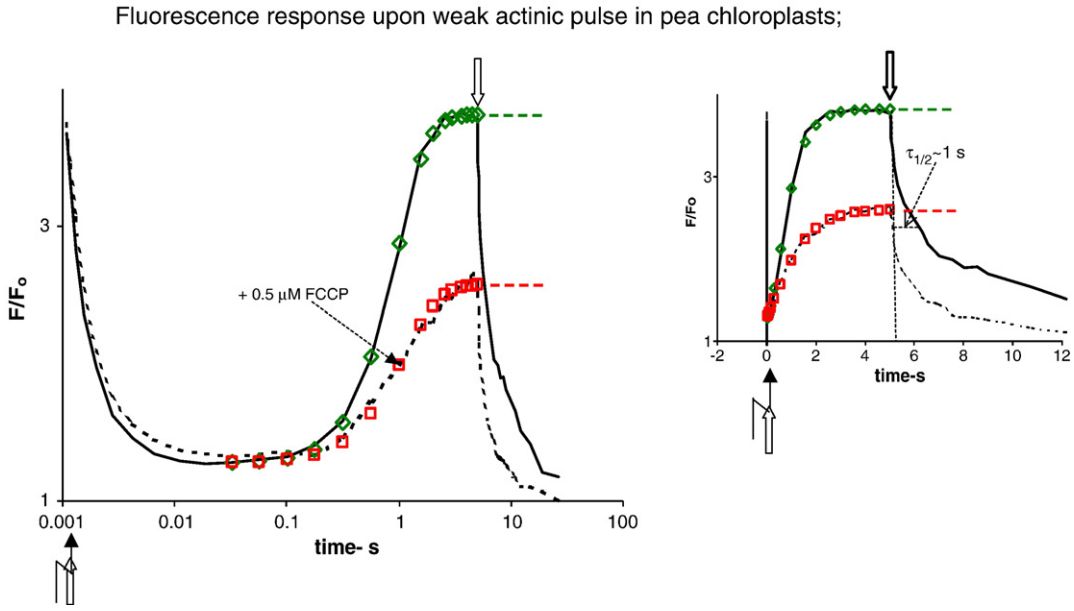

Fig. 2. $F(t)/F_o$ response upon simultaneous onset of a STF (STF_1) and a low intensity 5 s actinic pulse with excitation rate $k_L \sim 10\ s^{-1}$ plotted on a log and linear time scale (left and right hand panel, respectively). Onset of STF_1 (zigzagged arrow) and actinic pulse (upward pointing open arrow) at $t=0$ were with a minimal delay of a few μs. Green open diamonds and red open squares are simulated $F(t)/F_o$ values in the presence and absence of 0.5 μM FCCCP calculated with $F^{PE}(t)$ (Eq. (1)). Parameter values in the absence of FCCCP were identical as those of Fig. 1, except for N and k_{qbf} which were 2 and 3, respectively. Parameter values in the presence of the protonophore were unaltered except for k_{qbf} and k_{-PE} which changed from 3 and 0.3 to 2 and 2.1, respectively. Note also that FCCP did not alter the $F(t)/F_o$ response upon STF_1.

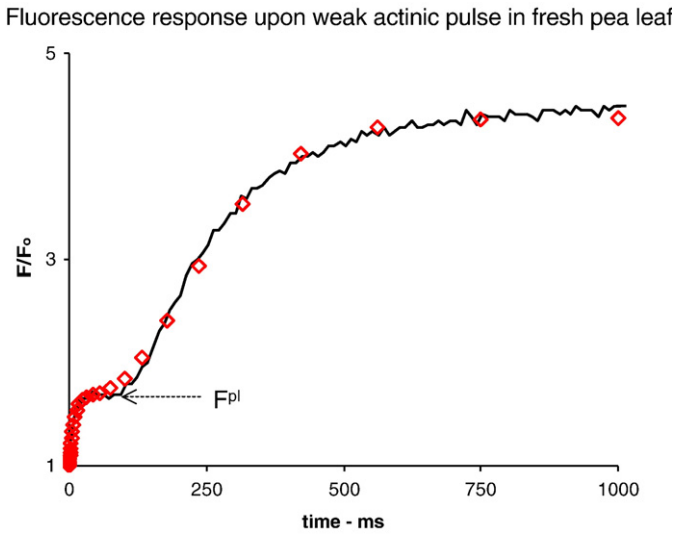

Fig. 3. Chlorophyll *a* fluorescence induction curve $F(t)/F_o$ of 10 min dark-adapted pea leaf upon 1 s MTF excitation at low excitation $k_L \sim 120\ s^{-1}$ plotted on a linear time scale (solid line). Red open diamonds are calculated with $F^{PE}(t)$ (Eq. (1)) for matching with the experimental curve in the 0–1 s time range. Matching parameters β, nF_v, N, k_{qbf} and k_{-PE} were 0.3, 2.7, 3 and (in s^{-1}) 14 and 0.3, respectively.

substantially reduced. Comparison of the *in silico* parameters supplied by application of the simulation function $F^{PE}(t)$ shows (see legend) that addition of the protonophore has caused an approx. seven fold increase in the rate constant k_{-PE} which represents the trans-thylakoid proton leak with hardly a change, if any in the other parameters, except for a slight decrease in the turnover rate k_{qbf} of the proton pump. It was found (data not shown) that doubling of the FCCP concentration causes a nearly complete inhibition of the $F(t)/F_o$ response in the weak actinic light. This result is in agreement with the inhibitory effect of the uncoupler on the response in a 12.5 Hz STF train [30,34].

Fig. 3 shows, for comparison the fluorescence response in an intact pea leaf upon a low intensity actinic pulse (intensity ~ 30 μmol photons $m^{-2}\ s^{-1}$ corresponding with $k_L \sim 0.12\ ms^{-1}$). This is at an approx. ten fold higher excitation rate than in the experiment of Fig. 2. Nevertheless the kinetic patterns are comparable: a rapid rise of $F(t)$ to a plateau F^{pl} (relative to F_o) followed by a retarded S-shaped rise towards a steady state, which at the tenfold higher intensity (excitation rate) is at $F_m/F_o \sim 4.5$.

Fig. 4 (a, upper part) shows the same experiment as illustrated in Fig. 2, except for the modification that the thylakoids have been excited with two additional STFs, one (STF_2) supplementary to the low intensity actinic pulse at $t = 3$ s and the other (STF_3) at $t = 9$ s during the dark period after the actinic light. The response illustrates that STF_2 causes a rapid increase in fluorescence emission (release of fluorescence quenching) towards a maximum $F_m \sim 5\ F_o$ which is substantially above the maximal $F_m \sim 3.8\ F_o$ induced by STF_1 and by

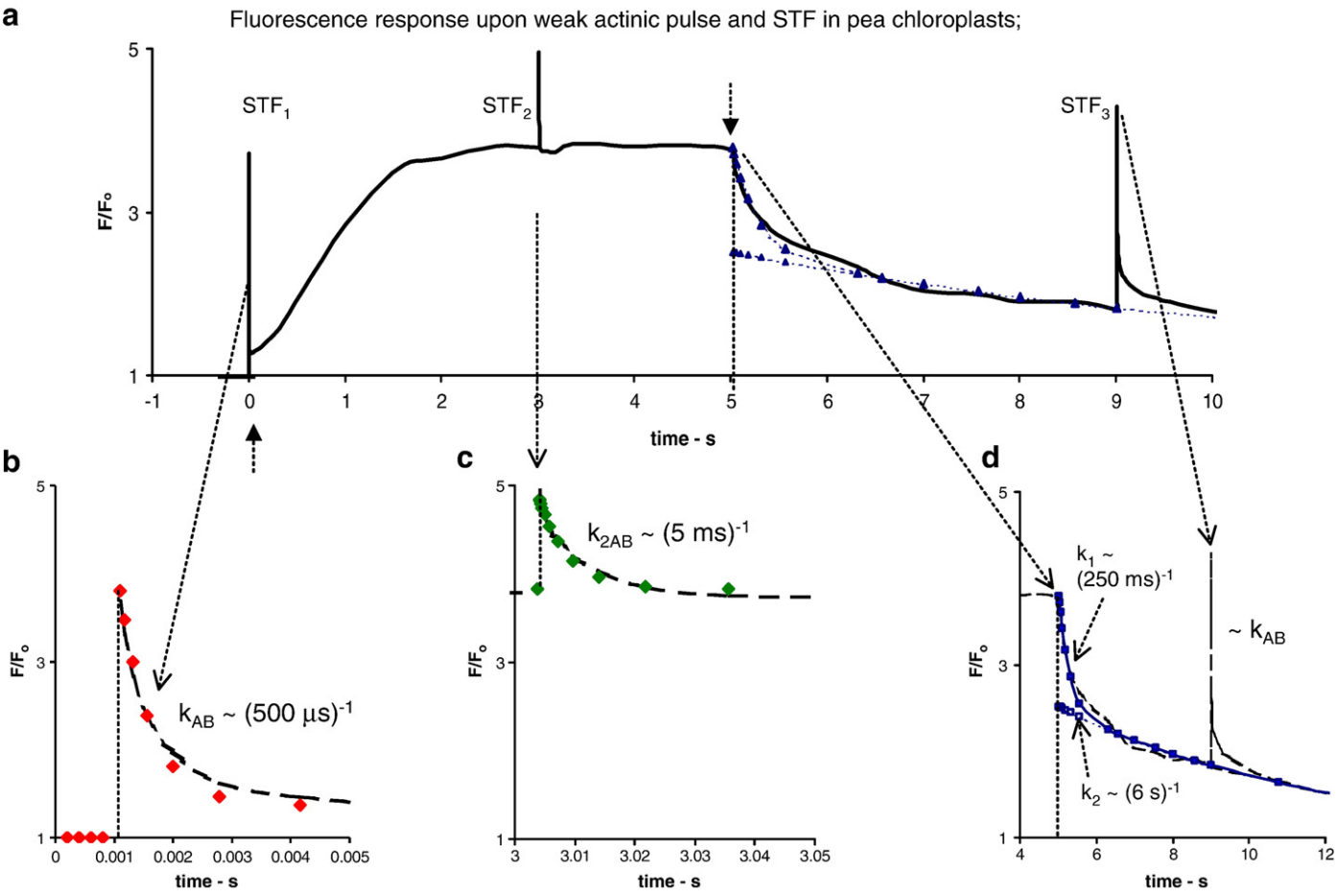

Fig. 4. (a) $F(t)/F_o$ response on a linear time scale in pea chloroplasts upon onset of a low intensity 5 s actinic MTF pulse with excitation rate $k_L \sim 10\ s^{-1}$ simultaneously with a train of 3 STFs fired at 0, 3 and 9 s. (b and c) Inzoom of STF_1- and STF_2-response with exponential fits (closed red and green diamonds, respectively) of dark decay with $k_{AB} \sim (500\ \mu s)^{-1}$ and $k_{2AB} \sim (5\ ms)^{-1}$, respectively. (d) same as b and c for the approx. bi-exponential decay after shutting of the actinic pulse at $t = 5$ s with rate constants $\sim (250\ ms)^{-1}$ and $\sim (6\ s)^{-1}$.

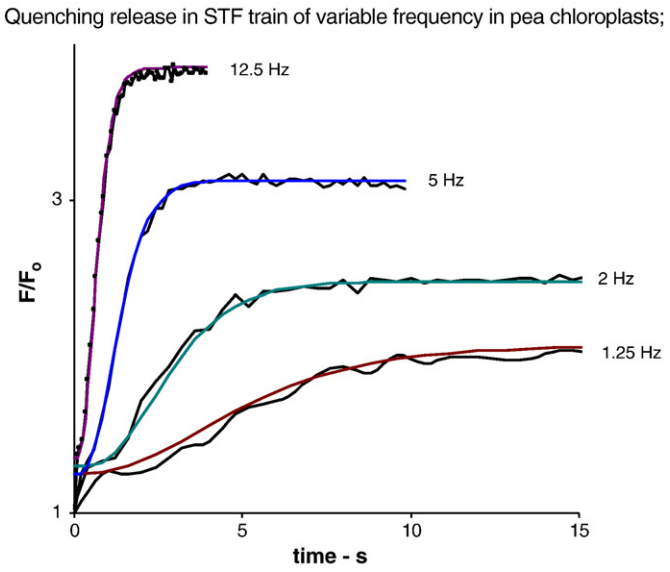

Fig. 5. Linear time courses (noisy curves) in 5–10 min dark-adapted pea chloroplasts of the $F(t)/F_o$ fluorescence level at the onset of subsequent STFs in trains of variable frequency in the range between 12.5 and 1.25 Hz. The solid lines are the curves calculated with the simulation function $F^{PE}(t)$ (Eq. (1)) and with k_L as variable parameter.

the low intensity actinic light. It also shows that the quenching recovery after shutting-off the actinic light is by several orders slower than after STF excitations. This is illustrated in detail in the lower part of the figure. The quenching recovery after STF_1 (Fig. 4b) with amplitude $F/F_o \sim 3.8$ occurs with rate constant $k_{AB} \sim (500\ \mu s)^{-1}$ indicating and confirming the association with (re-)oxidation of Q_A^- by Q_B (and Q_B^-). Quenching recovery after STF_2 (Fig. 4c) with amplitude $\Delta F/F_o \sim 1.2$ is 10 times slower and occurs with rate constant $k_{2AB} \sim (5\ ms)^{-1}$. This is in agreement with earlier results obtained with application of TTFs and STF trains in fluorescence studies [32]. The increment in and the recovery of the fluorescence response upon a TTF as compared to that upon an STF has been interpreted to originate from (re-) oxidation of the double-reduced acceptor pair $[Q_APhe]^{2-}$ after double excitation of electron trapping-competent RCs [34]. Recovery of the quenching after actinic light (Fig. 4d) is bi-exponential with rate constant $(0.25\ s)^{-1}$ and $(6\ s)^{-1}$ of components with comparable amplitude. The decay pattern is in agreement with that after a flash train and has been interpreted to originate from oxidation and recovery of accumulated single reduced Q_B-nonreducing open RCs [30]. The STF_3 response is similar to that of STF_1 (details not shown).

Fig. 5 shows, for STF trains with frequencies between 1.25 and 12.5 Hz, the response curves of the variable fluorescence at the onset of the subsequent STFs in each of the trains and their matching simulations using Eq. (1) with rate constant k_{qbf} proportionally tuned at the frequency of the train. The figure shows, in agreement with an earlier report [30] that the S-shaped rise of the variable fluorescence decreases with decrease in frequency of the STF train.

Fig. 6a (left hand panel) illustrates the different S-shapes of the relative variable fluorescence rFv in weak actinic light ($k_L \sim 3\ s^{-1}$) simulated (Eqs. (1) and (2)) for different values of the number N of buffering groups near the Q_B-binding site of the D1-protein (Appendix A). For simplicity the fraction of Q_B-nonreducing RCs at $t=0$ and the passive trans-thylakoid proton leak have been assumed to be zero ($\beta_o=0$ and $k_{-PE}=0$, respectively in Eq. (2)). Fig. 6b (right hand panel) shows, for N-values in the range between 0 and 5, rF_v^{PE} as function of fraction q^{PE} of RCs with 100% photoelectrochemical quenching qPE. The fraction q at each corresponding value rFv was estimated as the fractional size of + the area above the rFv(t) curve in the time interval t starting at $t=0$ (see also legend). The dashed curve through closed red triangles is the hyperbolic rFv – q relation $rFv = \frac{q}{1 + p.nF_v.(1-q)}$ [46] when the non-linearity is assumed to be caused by intersystem connectivity with $p=0.55$, q the fraction of RCs in which Q_A is reduced and $nF_v=2$ as has been proposed by others [47].

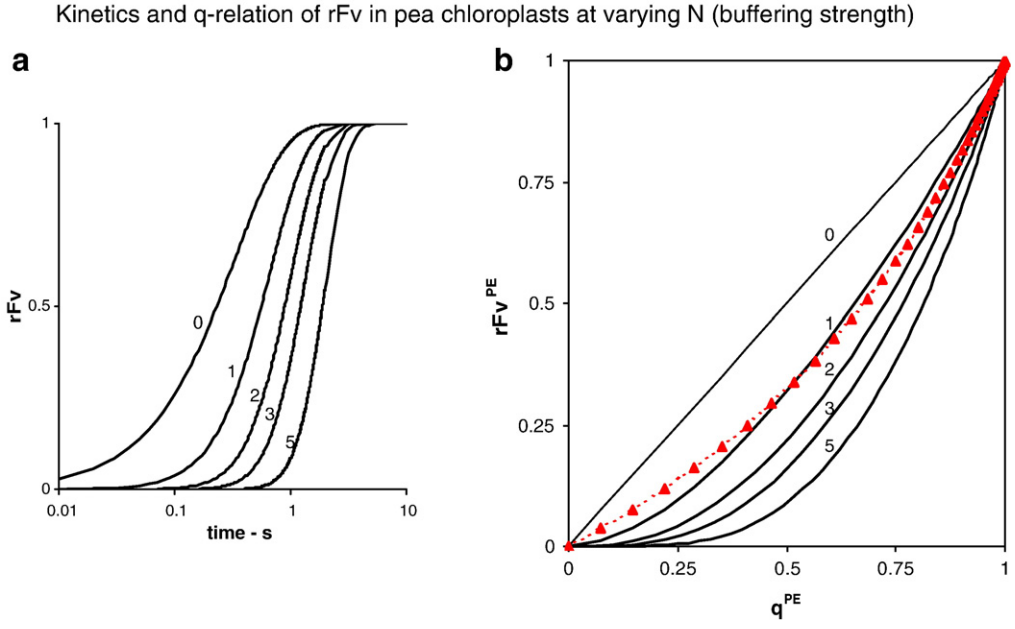

Fig. 6. (a) The relative variable fluorescence in low intensity MTF excitation $rFv(t)=1-qPE(t)$ on a logarithmic function of time (in s) calculated for a variable number (N) of buffering groups near the Q_B-binding site and using Eq. (1) with (from top to bottom $N=0, 1, 2, 3$ and 5; $k_{qbf}=3$, kmin = 0 and $b=0$. Note that the curve for $N=2$ is identical to the simulated curve in Fig. 2 in the absence of FCCP. (b) rFv plotted as a function of the fraction q of RCs with Q_A^- which under the condition of low intensity MTF excitation equals the fraction q^{PE} of RCs with qPE = 0. Fraction q^{PE} is the area above the normalized fluorescence induction curve $rF_v(t)=1-qPE(t)$ given in a. and is determined after substitution Eq. (A.3) in $q^{PE}(t) = \frac{\int_t^\infty qPE(t)dt}{\int_0^\infty qPE(t)dt}$ for a variable number (N) of buffering groups near the Q_B-binding site. N-numbers are as in a. For $N=0$ qPE and q^{PE} are linearly related. Note the increase in delay and steepness of the relation with increase in buffering strength. The dashed curve through closed red triangles is the rFv – q relation $rFv = \frac{q}{1 + p^*nF_v(1-q)}$ when the non-linearity is assumed to be caused by intersystem connectivity with $p=0.55$ and $nF_v=2$ as has been proposed by others [44].

Fig. 7 shows simulation curves which fit the trace connecting the fluorescence levels at onset of the STFs in a 12.5 Hz flash train in atrazine-sensitive (S-) and -resistant (R) thylakoids isolated from *Chenopodium album* leaves on a linear time scale (similar as curve with green symbols for pea thylakoids in Fig. 1). Simulation was done applying Eq. (2) with values for k_{qbf}, k_{-PE} (in s^{-1}) and N equal to 4, 0.1 and 6 for S-type and 1.3, 0.03 and 3 for R-type. The right hand panel shows the first derivative of these qPE(t) curves.

4. Discussion

The results illustrated in Figs. 1–4 show, in agreement with an earlier hypothesis [48], that changes in chlorophyll fluorescence yield accompanying the initial events at the onset of photochemical activity in the photosynthetic system can be the result of at least two distinguishable quenching processes. A change in fluorescence yield at a constant electrochemical potential is ascribed to (a change in) primary photochemical quenching. Conversely a change in fluorescence yield occurring at a constant activity of the primary photochemical reactions in the reaction center is associated with photoelectrochemical control of the electron transport at the acceptor side of PSII.

The onset of low intensity actinic light causes, after a distinct delay of 150 to 250 μs at a low plateau $F^{pl} \sim (0.3–0.5)^* F_o$, a sigmoid increase in fluorescence yield towards a steady state which, at the intensity used is reached after about 2 s (Figs. 2 and 3). Its amplitude at the intensity used is nearly equal to that of the STF_1-induced variable fluorescence nF_V^{STF1} and corresponds, with $k_L \sim 3\ ms^{-1}$, to a more than three-fold increase of fluorescence yield (relative to F_o). The recovery of this variable fluorescence in the dark occurs with a half time of approx. 1 s and is more than 10^3 times slower than that of nF_V^{STF1}. The reaction pattern in low intensity light and in the dark shows close similarities with that of the variable fluorescence measured 80 ms after single turnover excitation in a 12.5 Hz train of 60 STFs (Fig. 1). The S-shaped rise pattern thereof has been discussed and evidenced to be associated with accumulation and reduction of Q_B-nonreducing RCs [30].

The weak intensity actinic light pulse used in the experiments of Figs. 2–4 does not effect the photochemical quenching. A release thereof at an excitation rate of the order of 0.01 ms^{-1} (= 10 s^{-1}) is counterbalanced by the much higher rate constant $k_{AB} \sim 2\ ms^{-1}$ of its recovery which is governed by the reoxidation of Q_A^-. Therefore, and in line with the hypothesis cited above, the increase in fluorescence in weak actinic light with $k_L < 0.1\ ms^{-1}$ can be ascribed to a release of photoelectrochemical quenching. A photoelectrochemical origin associated with accumulation and reduction of Q_B-nonreducing RCs was indeed concluded for the comparable rise pattern in STF trains like the one shown in Fig. 1 [30]. Accumulation of this type of RCs has been discussed to result from the alkaline shift of the of the $Q_A^- Q_B \leftrightarrow Q_A Q_B^-$ equilibrium in conjunction with trans-thylakoid proton transport into the lumen powered by the proton motive Q cycle. The coupling with proton transfer was substantiated by the pronounced effects of the protonophore FCCP and of valinomycin [30]. The decrease in the quenching release in weak intensity actinic light in the presence of 0.5 μM FCCP is due to an approx. seven fold increase in the passive proton leak of the thylakoid as reflected by the increased rate constant k_{-PE} in the simulation. The slow recovery of photoelectrochemical quenching, i.e. the slow disappearance of Q_A^- in the dark is in agreement with an earlier conclusion that this type of quenching is associated with Q_B-nonreducing RCs. The unaltered kinetics of variable fluorescence upon STF excitation (STF_1) in absence and presence of FCCP (Fig. 2) confirm earlier results [30,34] that the protonophore does not affect photochemical quenching.

Additional evidence for the conclusion that the fluorescence increase in a weak 4 s MTF pulse originates from a quenching mechanism different from that of photochemical quenching comes from the fluorescence response upon a second flash (STF_2) fired at $t = 3$ s during the MTF pulse (Figs. 4a, d). Notwithstanding the fact that the fluorescence signal in the low intensity light has risen towards a level $F \sim 3.8$, which suggests complete photochemical reduction of the quencher Q_A, STF_2 causes a complementary transient increase in variable fluorescence towards $F \sim 5$ (relative to F_o). The recovery of the STF_2-induced fluorescence response (Fig. 4 d) is distinctly slower than that induced by STF_1 and occurs with a rate constant of about $(5\ ms)^{-1}$. These kinetics show strong and convincing similarities with those observed as components of the ones upon excitation with STF-twins (TTF) or -trains [34, see also

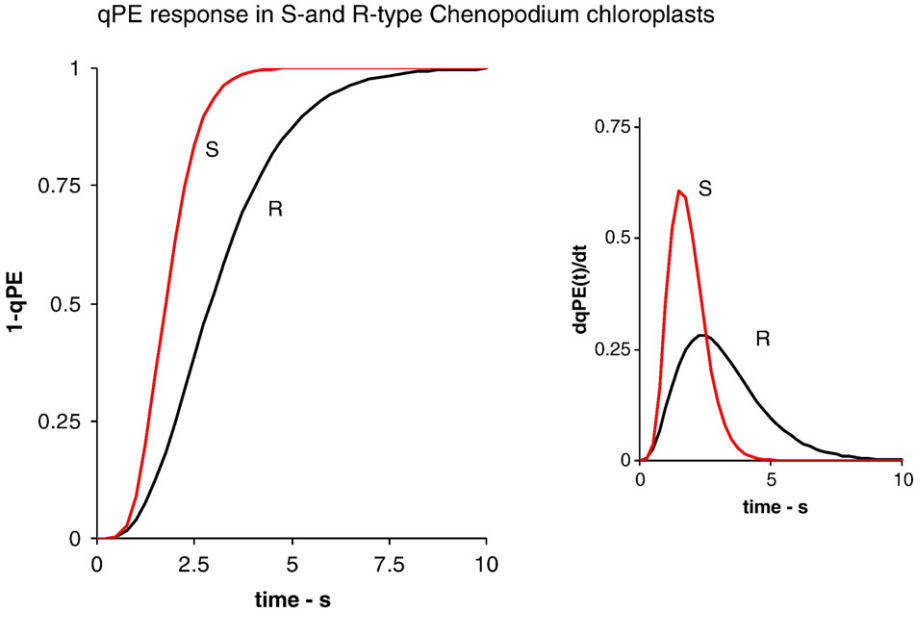

Fig. 7. Simulation curves of experimental fluorescence data points which connect the fluorescence levels at the onset of the STFs in a 12.5 Hz flash train in S- and R-type thylakoids isolated from atrazine-sensitive and -resistant *Chenopodium album*, respectively on a linear time scale (similar as curve with green symbols shown for pea thylakoids in Fig. 1). Simulation was done applying Eq. (2) with values for k_{qbf}, k_{-PE} (in s^{-1}) and N equal to 4, 0.1 and 6 for S-type and 1.3, 0.03 and 3 for R-type. The right hand panel shows the first derivative of these qPE(t) curves.

Fig. 1]. The response is attributed to electron trapping and release of photochemical quenching in Q_B-nonreducing RCs that have accumulated and become reduced in the actinic pulse. This trapping results in double reduction of the PS II acceptor pair [$PheQ_A$]. The subsequent quenching recovery reflects the (single) reoxidation of $[PheQ_A]^{2-}$ in these RCs.

Some of the responses shown in Figs. 1–4 are reproduced and summarized in Fig. 8. They illustrate and indicate that primary photochemical quenching occurs independent of and is additive to photoelectrochemical quenching. This is the first demonstration of the separate effect of both types of quenching release occurring at the onset of illumination of a dark-adapted system. The summed effect results in a variable fluorescence $F_v \sim 4\ F_o$ corresponding with $F_v/F_m^{MTF} \sim 0.8$. Usually and commonly as a routine a high fluorescence signal F_m ($=F_m^{MTF}$) is reached with saturation pulse-induced fluorescence analysis (like in PAM fluorometers [49]) using a high intensity light pulse of ~300 ms duration and is ascribed to the release of photochemical quenching designated with the coefficient (or index) of photochemical quenching qP (for review see [50]). Our results show that the hitherto called photochemical quenching release of a dark-adapted system, associated with a fluorescence increase from F_o to F_m and $F_v/F_m \sim 0.8$, has to be considered as a composite and complementary release of primary photochemical (PP) and photoelectrochemical (PE) quenching, which we will designate with qPP and qPE, respectively. The quenching state of a system during an MTF illumination protocol towards its maximum level F_m will be characterized with a vector (qPP,qPE) with qPP and qPE variable between 0 and 1. Full quenching release changes the dark-adapted quenching state from (qPP,qPE) = (1,1) to (0,0) at F_o and F_m^{MTF}, respectively and release of photochemical and photoelectrochemical from (qPP,qPE) = (1,1) to (0,1) and (1,0) at F_o and F_m^{STF} respectively.

Fig. 8 visualizes the resolution of what till now has been characterized as photochemical quenching qP into a 'primary' photochemical quenching part qPP complemented with a photoelectrochemical component qPE. It is assumed that i) the dark-adapted quenched state (qPP,qPE) = (1,1) is heterogeneous with S_0/S_1 fraction ratio $\beta_o/(1-\beta_o)$ [51], and ii) the release of qPP and qPE at qPE = 1 and qPP = 1, respectively is associated with a normalized variable fluorescence $nF_v^{STF} = nF_v^{PP} = nF_v^{PE} = 2$. A quenching release with $nF_v^{STF} \sim 2$ is commonly found upon STF excitation [30,34]. The results illustrated in Fig. 1 (and in Figs 2 and 4), where release of qPP and qPE induced by $STF_1$and low intensity actinic light, respectively is associated with $nF_v^{STF} > 2$ seem to be a little at variance with this assumption based on earlier results. The aberration is probably caused by the use of the new high intensity version of the PSI fluorometer with consequently too high a photon flux (intensity) in STFs in the present experiments. This may have caused an increased probability of double hits and double reduction of Q_B-nonreducing RCs with concomitant increase in F above $nF_v^{STF} \sim 2$ [34]. STF excitation (STF_1 in Fig. 4) causes transient release of quenching from (qPP,qPE) = (1,1) to (0,1) attributed to qPP and associated with $nF_v^{STF} \sim 2$. Recovery of this release at (qPP,qPE) = (0,1) occurs with rate constant ~ $(500\ \mu s)^{-1}$ towards a quasi-steady state $F^{pl} = 1 + \beta_o * nF_v^{STF}$ (Fig. 4). Actinic illumination of low intensity (excitation rate $\ll 0.1\ ms^{-1}$) causes a monotonic rise (not resolved) to

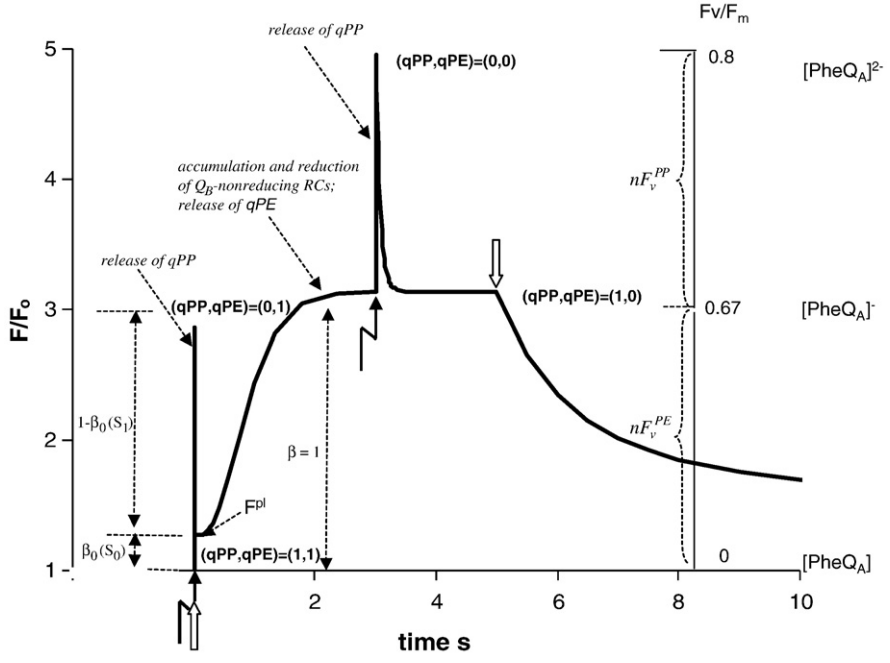

Fig. 8. Schematic reconstruction (based on data of Figs. 1–4) of the experimental fluorescence response in 5–10 min dark-adapted pea thylakoids, plotted as $F(t)/F_o$ on a linear time scale, upon a weak intensity (~3 μE photons $m^{-2}\ s^{-1}$) 5 s actinic light pulse (up- and downward open arrow) supplemented with two saturated single turnover 35 μs flashes (STF), fired at time $t = 0$ and $t = 3$ s (zigzagged arrows). The intensity of the actinic light corresponds with an excitation rate $k_L \sim 0.01\ ms^{-1}$. The first flash at $t = 0$ (STF_1) causes the approx. two-fold increase in variable fluorescence (relative to F_o) with a rapid decay (unresolved on this time scale, but occurring with rate constant $k_{AB} \sim (0.5\ ms)^{-1}$) towards a quasi-steady state level, called F^{pl}, with in this case $F^{pl}/F_o \sim 1.3$. This response results from release and recovery of photochemical quenching denoted with qPP. F^{pl} originates from non-quenched fluorescence of the β_0-fraction, probably identical with the S_0 fraction with Q_B-nonreducing RCs. The weak actinic light causes, after a distinct delay of 200 to 250 μs a sigmoid increase in fluorescence towards a steady state which, at the intensity used is reached after about 2 s. Its size corresponds roughly with a two-fold increase in variable fluorescence (relative to F_o). The increase in fluorescence in weak actinic light, which does not effect the photochemical quenching (see text), is ascribed to release of photoelectrochemical quenching qPE associated with accumulation and reduction of Q_B-nonreducing RCs. The slow recovery of photoelectrochemical quenching, i.e. the slow disappearance of Q_A^- in the dark occurs with a half time of approx. 2 s and is in agreement with an earlier conclusion that this type of quenching is associated with Q_B-nonreducing RCs. The second flash fired at $t = 3$ s (STF_2) causes, like STF_1, an approx. two-fold increase in variable fluorescence (relative to F_o). It is superimposed on the variable fluorescence in the weak actinic light (qPE = 0) and causes a maximal fluorescence with $F(t)/F_o \sim 5$. The recovery of the STF_2 response is distinctly slower than that induced by STF_1 and occurs with a rate constant of about $(6\ ms)^{-1}$. The summed effect of qPP- and qPE-quenching release results in a variable fluorescence $F_v \sim 4F_o$ corresponding with $F_v/F_m \sim 0.8$, which in PAM-vocabulary has been ascribed to the release of photochemical quenching qP [49]. Here we show that quenching of a dark-adapted system originates from photochemical qPP and photoelectrochemical quenching qPE. The quenching state of the system during an illumination protocol us designated with a vector (qPP,qPE) with qPP and qPE variable between 0 and 1. Full quenching release will change the dark-adapted quenching state from (1,1) to (0,0); release of photochemical and photoelectrochemical from (1,1) to (0,1) and (1,0), respectively.

F^{pl} within some tens of ms (Fig. 3) followed by an S-shaped rise $F^{PE}(t)$ ascribed to release of qPE quenching from (qPP,qPE) = (1,1 − β_o) to (1,0). This quenching release, associated with accumulation and reduction of Q_B-nonreducing RCs, occurs with amplitude $nF_v^{STF} \sim 2$ and is completed within a few s. STF excitation (STF_2 in Fig. 4) of the system kept in the 'semi-quenched' steady state with (qPP,qPE) = (1,0) causes a transient release of qPP towards a 'non-quenched' state (qPP,qPE) = (0,0) with $F = F_m \sim F_o + 2 * nF_v^{STF} = 5 * F_o$. Recovery of the STF-induced qPP quenching release at (qPP,qPE) = (0,0) occurs with rate constant ~(5 ms)$^{-1}$, ascribed to that of (single) oxidation of double-reduced Q_B-nonreducing RCs [30]. The half time of the qPE quenching release at (qPP,qPE) = (1,0) is about 1 s (Fig. 2). At full quenching release with (qPP,qPE) = (0,0), $F_v/F_m \sim 0.8$ which is the value that commonly is found in healthy thylakoid preparations when the PAM technology with saturating high intensity pulses of a few hundred ms duration is applied.

The kinetics of qPE release qPE(t) at qPP = 1 can be derived at low intensity MTF excitation from the $F(t) = F^{PE}(t)$ response, as illustrated in Figs. 1, 2 and 8. The analytical expression of $q^{PE}(t)$ is given by Eq. (2) (see also Appendix A.1). Constraints on the intensity of the actinic light (excitation rate k_L which at low value is assumed to be of the order of that of the proton pumping k_{qbf}) that have to be taken into account to prevent effects of interference of qPE with qPP and trans-thylakoid proton leak k_{-PE} are given in the Appendix A.2. It is shown that the kinetics of qPE release can be measured with less than 5% interference with qPP and reversion of qPE only for a narrow intensity range $8 \leq k_L \leq 10\ s^{-1}$. The constraint on the lower limit of k_L is confirmed and illustrated in Fig. 5. This shows the decline of the amplitude of $F(t)/F_o$ responses in STF trains at frequencies below 10 Hz. The dependency of qPE(t) on the proton leak through the thylakoid membrane k_{-PE} (Eq. (2)) is in qualitative agreement with the experimental and simulated FCCP-dependent fluorescence response in low intensity actinic light (Fig. 2). The simulation showed that the FCCP-induced change of the response is caused by a substantial increase in k_{-PE}. This is what would be expected for the action of a protonophore like FCCP.

There is as yet no direct validation for the dependency (Eq. (2)) of qPE(t) on, the number N of buffering groups near the Q_B-binding site. An increase in N, as illustrated graphically in Fig. 6, will cause an increase in the delay and steepness of $rFv^{PE}(t)$ which at low intensities is equivalent with 1-qPE(t). However, experiments with thylakoids isolated from atrazine-sensitive (S) and -resistant (R) *Chenopodium* plants and similar as those illustrated in Fig. 1 for pea thylakoids, have shown marked difference in their qPE(t) responses which might be related to different electrochemical properties around the Q_B-binding site in these genotypes [44]. The simulations of their qPE(t) response, using Eq. (2) and illustrated in Fig. 7, showed that the values of N were 6 and 3 in S- and R-plants, respectively. The reduced steepness of the rise in R-plants, associated with lower N, as compared with the wild type S-plants, is graphically illustrated in the graph of the respective qPE(t) derivatives (right hand panel of Fig. 7). The suggested association of N with the number of buffering groups in the phase near the Q_B-binding site then would indicate that the consequence of mutation of this site, which has amply been documented to be accompanied by a shift of the $Q_A^- Q_B \leftrightarrow Q_A Q_B^-$ redox equilibrium [52,53], is also found in a change in the buffering capacity of its adjacent phase. The results of Fig. 6 exclude evidence for the alternative interpretation [47] that the sigmoid kinetics of the variable fluorescence at low intensities of exciting light can be understood in terms of intersystem connectivity.

The present results contribute to the ongoing debate regarding the origin of the so-called 'thermal' J-(D)-I-P-phase of the MTF-induced response of variable fluorescence (see [24,33] for reviews). A common view, but challenged [54], is that this phase is associated with the progressive reduction of the acceptor side of PSII, notably the reduction of the PQ pool. Here the evidence is presented for the conclusion that the thermal phase, which after normalization is likely to resemble the qPE(t) curve measured at low intensities, is associated with trans-membrane proton transport that is electrochemically coupled to PQ reduction. The particular kinetics of the J-I phase with an S-shaped steep rise after a pronounced delay and analytically described by Eq. (2), would be difficult to bring in harmony with PQ being a quencher. Moreover the sensitivity of this phase to the protonophoric action of FCCP (Fig. 2) which is in agreement with earlier results and which were interpreted to indicate an electrochemical origin of the thermal phase [30], is also inconclusive with PQ acting as the quencher.

Further experiments are required to determine the relevance of what we call primary photochemical (qPP) and photoelectrochemical (qPE) quenching on existing views and interpretation models of so-called non photochemical quenching (NPQ). NPQ with its energetic-(qE), photoinhibitory-(qI) and state transition-(qT) related quenching components comes into expression during the PSTM fluorescence decline after F_m in prolonged illumination (see [55] for a recent review). The qE quenching component certainly will require a thorough re-evaluation. The currently adopted notion that the maximal variable fluorescence at F_m with (qPP,qPE) = (0,0) is associated exclusively with a release of photochemical quenching and gives a measure of the intrinsic photochemical yield q_p of PSII [55,56] that is susceptible to qE quenching, cannot easily be brought in harmony with the present results. It remains to be established whether or not our hypothesis that qE quenching is the inverse of the release of photoelectrochemical quenching qPE is true.

Acknowledgements

This research was supported by the Ministry of Education of the Czech Republic (Research concept MSM6007665808), by the Academy of Sciences of the Czech Republic (Research concept AV0Z50200510) and by the Grant Agency of the Czech Republic (Project 206/08/1683). We thank J. Hunalova for isolation and preparation of thylakoids.

Appendices

A. Derivation of expressions (Eqs. (1),(2)) that describe the kinetics of the release of photoelectrochemical quenching qPE in terms of the rate of trans-thylakoid proton pumping and leak and of the number of proton binding sites in (of) the cytbf protein complex

The delayed and S-shaped increase in variable fluorescence at low intensities (excitation rate) starting from a plateau level F^{pl}, which is determined by the fraction β_o of Q_B-nonreducing RCs in dark-adapted samples, can analytically be described in terms of a simple model that can be thought of as follows.

The increase in fluorescence yield at full (and unaltered) photochemical quenching qPP = 1 with $F = F_o$, ignoring the relatively small release of qPP with $\Delta qPP = \beta_o$, occurs in response to ΔpH in the vicinity of the Q_B-binding site of the D1-protein at the luminal side of the thylakoid membrane. The pH shift causes the $Q_A^- Q_B \leftrightarrow Q_A Q_B^-$ redox equilibrium to move to the $Q_A^- Q_B$ direction. It will happen in association with trans-thylakoid proton transfer upon onset of the Q-cycle driven proton pump in the cytbf complex after photochemical electron trapping at the acceptor side of PS II. We designate the electrochemical potential of the phase adjacent to the binding site after n turnovers of PS II (and the Q cycle) with μ_n(pH) (n = 0,1, 2, etc). The delayed and S-shaped fluorescence rise at qPP = 1 suggests that the pH associated with μ_n(pH) is dependent on the number of turnovers of PS II (and pump) with a delayed and S-shaped profile. The transfer of the states can be symbolized and represented by the scheme

$$\mu_0(\mathrm{pH}) \xrightarrow{k_{qbf}} \mu_1(\mathrm{pH}) \xrightarrow{k_{qbf}} \ldots\ldots \xrightarrow{k_{qbf}} \mu_{N-1}(\mathrm{pH}) \underset{k_{-PE}}{\overset{k_{qbf}}{\Leftrightarrow}} \mu_N(\mathrm{pH} + \Delta\mathrm{pH}) \qquad (A.1)$$

in which k_{qbf} and k_{-PE} are rate constants of proton pumping and proton leak through the thylakoid membrane, respectively. At low intensities the pumping rate is assumed to be equal to the light excitation rate $k_{qbf} \sim k_L$. $\mu_n(pH)$ symbolizes the assumption that the electrochemical potential μ_n is predominantly determined by the actual pH. The scheme can be read as that of a process in which N protons have to be delivered to or extracted from an aqueous phase before a change in pH will occur. N then can be viewed as the number of proton buffering groups in that phase. The $[N+1]$ differential equations associated with the reaction scheme can be numerically solved by an adopted matrix solver method for ODEs (see for details [23,35] and approximated analytically [57] yielding

$$\mu_N(t) = \mu_0 + (\mu_N^{ss} - \mu_0)\left(1 - e^{-k_{qbf}\cdot t}\sum_{m=0}^{N}\frac{\left(k_{qbf}t\right)^m}{m!}\right)\frac{k_{qbf}}{k_{qbf} + k_{-PE}} \tag{A.2}$$

in which μ_N^{ss} equals $\mu_N(t)$ in the final steady state. The approximation equals the analytical solution of the ODEs in case the passive proton leak is ignored ($k_{-PE}=0$) and can be shown to hold within maximal 10% deviation for $k_{-PE} < 2.k_{qbf}$. After normalization with reference to the electrochemical potential $\mu_0(pH)$ and μ_N^{ss} in the dark-adapted (qPE = 1) and light equilibrium state (qPE = 0), respectively, the expression for qPE is

$$qPE(t) = \frac{\mu_N(t) - \mu_0}{\mu_N^{ss} - \mu_0} - 1 = e^{-k_{qbf}\cdot t}\sum_{m=0}^{N}\frac{\left(k_{qbf}t\right)^m}{m!})\frac{k_{qbf}}{k_{qbf} + k_{-PE}}. \tag{A.3}$$

B. Constraints for excitation rate k_L to prevent interference between qPE and qPP

Less than 5% interference of a qPE response with (release of) photochemical quenching (qPP) is guaranteed when the following condition is met:

$$\frac{k_L}{k_L + k_{AB}}\left(1 - e^{-(k_L + k_{AB})t}\right) \leq 0.05.$$

This yields $k_L \leq 0.01\ ms^{-1}$, for $k_{2AB} \sim (5\ ms)^{-1}$, i.e. the slowest rate constant of the qPP recovery in STF_2 (Fig. 4).

On the other hand if the extent of qPE should be less than 5% below the maximum then, in approximation and with $k_{qbf} = k_L$,

$$\frac{k_L}{k_L + k_{-PE}}\left(\left(1 - e^{-(k_L + k_{-PE})t}\right) \geq 0.95\right.$$

in which k_{-PE} is the rate constant of the reversal of qPE. After substitution of $k_{-PE} \sim (250\ ms)^{-1}$ (Fig. 4) one gets $k_L \geq 0.008\ ms^{-1}$. Thus there is, at least for thylakoids under the conditions used, a relative small range of excitation rate k_L ($0.008 \leq k_L \leq 0.01$) at which nearly full release of photoelectrochemical quenching qPE can be measured with less than 5% interference with qPP and attenuation due to reversion of qPE.

References

[1] B. Ke, in: Govindjee (Ed.), Photosynthesis Photobiochemistry and Photobiophysics. Advances in Photosynthesis and Respiration, Vol. 10, Kluwer Academic Publisher (now Springer), Dordrecht, 2001.

[2] Govindjee, Chlorophyll a fluorescence: a bit of basics and history, in: G. Papageorgiou, Govindjee (Eds.), Chlorophyll a Fluorescence: A Signature of Photosynthesis, Advances in Photosynthesis and Respiration, Vol. 19, Springer, Dordrecht, the Netherlands, 2004, pp. 1–42.

[3] G. Papageorgiou, Govindjee (Eds.), Chlorophyll a Fluorescence A Signature of Photosynthesis, Advances in Photosynthesis and Respiration, volume 19 (ISBN 1-4020-3217-X), Springer, Dordrecht, the Netherlands, 2004.

[4] W.J. Vredenberg, L.N.M. Duysens, Transfer and trapping of excitation energy from bacteriochlorophyll to a reaction center during bacterial photosynthesis, Nature 197 (1963) 355–357.

[5] P. Joliot, A. Joliot, Evidence for a double hit process in photosystem II based on fluorescence studies, Biochim. Biophys. Acta 462 (1977) 559–574.

[6] H. Dau, Molecular mechanisms and quantitative models of variable photosystem II fluorescence, Photochem. Photobiol. 60 (1994) 1–23.

[7] H.-W. Trissl, J. Lavergne, Fluorescence induction from photosystem II: analytical equations for the yields of photochemistry and fluorescence derived from analysis of a model including exciton-radical pair equilibrium and restricted energy transfer between photosynthetic units, Austral. J. Plant Physiol. 22 (1995) 183–193.

[8] U. Schreiber, A. Krieger, Hypothesis: two fundamentally different types of variable chlorophyll fluorescence in vivo, FEBS Lett. 397 (1996) 131–135.

[9] A.D. Stirbet, B. Govindjee, J. Strasser, R.J. Strasser, Chlorophyll *a* fluorescence induction in higher plants: modeling and numerical simulation, J. Theor. Biol. 193 (1998) 131–151.

[10] K. Bernhardt, H.-W. Trissl, Theories for kinetics and yields of fluorescence and photochemistry: how, if at all, can different models of antenna organization be distinguished experimentally? Biochim. Biophys. Acta 1409 (1999) 125–142.

[11] W.J. Vredenberg, A three state model for energy trapping and chlorophyll fluorescence in photosystem II incorporating radical pair recombination, Biophys. J. 78 (2000) 25–38.

[12] Xin-Guang Zhu, Govindjee, N.R. Baker, E. deSturler, D.R. Ort, S.P. Long, Chlorophyll *a* fluorescence induction kinetics in leaves predicted from a model describing each discrete step of excitation energy and electron transfer associated with Photosystem II, Planta 23 (2005) 114–133.

[13] D. Lazár, The polyphasic chlorophyll a fluorescence rise measured under high intensity of exciting light, Funct. Plant Biol. 33 (2006) 9–30.

[14] N.E. Belyaeva, F.-E. Schmitt, R. Steffen, V.Z. Paschenko, G. Yu Riznichenko, Yu K. Chemeris, G. Renger, A.B. Rubin, PS II model-based simulations of single turnover flash-induced transients of fluorescence yield monitored within the time domain of 100 ns–10 s on dark-adapted *Chlorella pyrenoidosa* cells, Photosynth. Res. 98 (2008) 105–119.

[15] A. Rubin, G. Riznichenko, Modeling of the primary processes in a photosynthetic membrane, in: A Laisk, L. Nedbal, Govindjee (Eds.), Photosynthesis In Silico: Understanding Complexity from Molecules to Ecosystems, Springer, Dordrecht (the Netherlands), 2009, pp. 151–176.

[16] L.N.M. Duysens, H.E. Sweers, Mechanisms of the two photochemical reactions in algae as studied by means of fluorescence, in: Japanese Society of Plant Physiologists (Ed.), Studies on Microalgae and Photosynthetic Bacteria, University of Tokyo Press, Tokyo, 1963, pp. 353–372.

[17] W.L. Butler, On the primary nature of fluorescence yield changes associated with photosynthesis, Proc. Natl. Acad. Sci. U. S. A. 69 (1972) 3420–3422.

[18] V.V. Klimov, A.A. Krasnovskii, Participation of pheophytin in the primary processes of electron transfer at the reaction centers of photosystem II, Biophysics 27 (1981) 186–198.

[19] D.M. Kramer, G. DiMarco, F. Loreto, Contribution of plastoquinone quenching to saturation pulse-induced rise of chlorophyll fluorescence in leaves, in: P Mathis (Ed.), Photosynthesis: From Light to Biosphere, Vol. I, Kluwer Academic Publishers, Dordrecht, The Netherlands, 1995, pp. 147–150.

[20] S. Vasilév, D. Bruce, Nonphotochemical quenching of excitation energy in photosystem II. A picosecond time-resolved study of the low yield of chlorophyll a fluorescence induced by single-turnover flash in isolated spinach thylakoids, Biochemistry 37 (1998) 11046–11054.

[21] J. Kurreck, R. Schödel, G. Renger, Investigation of the plastoquinone pool size and fluorescence quenching in thylakoid membranes and Photosystem II (PSII) membrane fragments, Photosynth. Res. 63 (2000) 171–182.

[22] M. Koblizek, D. Kaftan, L. Nedbal, On the relationship between the non-photochemical quenching of the chlorophyll fluorescence and the photosystem II light harvesting efficiency. A repetitive flash fluorescence study, Photosynth. Res. 68 (2001) 141–152.

[23] W.J. Vredenberg, System analysis and photo-electrochemical control of chlorophyll fluorescence in terms of trapping models of photosystem II: a challenging view, in: G. Papageorgiou, Govindjee (Eds.), Chlorophyll a Fluorescence: A Signature of Photosynthesis, Advances in Photosynthesis and Respiration, Vol. 19, Springer, Dordrecht, the Netherlands, 2004, pp. 133–172.

[24] G. Samson, O. Prasil, B. Yaakoubd, Photochemical and thermal phases of chlorophyll a fluorescence, Photosynthetica 37 (1999) 163–182.

[25] G.C. Papageorgiou, M. Tsimilli-Michael, K. Stamatakis, The fast and slow kinetics of chlorophyll a fluorescence induction in plants, algae and cyanobacteria: a viewpoint, Photosynth. Res. 94 (2007) 275–290.

[26] G. Samson, D. Bruce, Origins of the low yield of chlorophyll fluorescence induced by single turnover flash in spinach thylakoids, Biochim. Biophys. Acta 1276 (1996) 147–153.

[27] Z.S. Kolber, O. Prasil, P.G. Falkowski, Measurements of variable chlorophyll fluorescence using fast repetition rate techniques. I. Defining methodology and experimental protocols, Biochim. Biophys. Acta 1367 (1998) 88–106.

[28] U. Schreiber, Assesment of maximalfluorescence yield: donor-side dependent quenching and QB-quenching, in: O. van Kooten, J. Snel (Eds.), Plant Spectrofluotometry: Applications and Basic Research, Rozenberg Publ., Amsterdam, 2002, pp. 23–47.

[29] W.J. Vredenberg, J.J.S. van Rensen, G.C. Rodrigues, On the sub-maximal yield and photo-electric stimulation of chlorophyll a fluorescence in single turnover excitations in plant cells, Bioelectrochem 68 (2005) 83–90.

[30] W.J. Vredenberg, V. Kasalicky, M. Durchan, O. Prasil, The chlorophyll a fluorescence induction pattern in chloroplasts upon repetitive single turnover excitations: accumulation and function of Q_B-nonreducing centers, Biochim. Biophys. Acta 1757 (2006) 173–181.
[31] W.J. Vredenberg, O. Prasil, Modeling of chlorophyll a fluorescence kinetics in plant cells: derivation of a descriptive algorithm, in: A. Laisk, L. Nedbal, Govindjee (Eds.), Photosynthesis In Silico: Understanding Complexity from Molecules to Ecosystems, Springer, Dordrecht (the Netherlands, 2009, pp. 125–140.
[32] R.J. Strasser, A. Srivastava, Govindjee, Polyphasic chlorophyll a fluorescence transient in plants and cyanobacteria, Photochem. Photobiol. 61 (1995) 32–42.
[33] D. Lazár, G. Schansker, Models of Chlorophyll a Fluorescence Transients, in: A Laisk, L. Nedbal, Govindjee (Eds.), Photosynthesis In Silico: Understanding Complexity from Molecules to Ecosystems, Springer, Dordrecht (the Netherlands), 2009, pp. 85–123.
[34] W.J. Vredenberg, M. Durchan, O. Prasil, On the chlorophyll fluorescence yield in chloroplasts upon excitation with twin turnover flashes (TTF) and high frequency flash trains, Photosynth. Res. 93 (2007) 183–192.
[35] M. Hiraki, W.J. Vredenberg, J.J.S. van Rensen, K. Wakabayashi, A modified fluorometric method to quantify the concentration effect (pI_{50}) of photosystem II-inhibiting herbicides, Pesticide Biochem. Physiol. 80 (2004) 183–191.
[36] W.J. Vredenberg, Kinetic models of photosystem II should incorporate a role for Q_B-nonreducing reaction centers, Biophys. J. 95 (2008) 3113–3114.
[37] A. Melis, Functional properties of photosystem IIβ in spinach chloroplasts, Biochim. Biophys. Acta 808 (1985) 334–342.
[38] R.A. Chylla, G. Garab, J. Whitmarsh, Evidence for slow turnover in a fraction of photosystem II complexes in thylakoid membranes, Biochim. Biophys. Acta 894 (1987) 562–571.
[39] J. Lavergne, E. Leci, Properties of inactive photosystem II centers, Photosynth. Res. 35 (1993) 323–343.
[40] M. Durchan, F. Vácha, A. Krieger-Liszkay, Effects of severe CO_2 starvation on the photosynthetic electron transport chain in tobacco plants, Photosynt. Res. 68 (2001) 203–213.
[41] L. Nedbal, M. Trtilek, D. Kaftan, Flash fluorescence induction; a novel method to study regulation of photosystem II, J. Photochem. Photobiol.B: Biol. 48 (1999) 154–157.
[42] W.J. Vredenberg, Algorithm for analysis of OJDIP fluoresecnce induction curves in terms of photo- and electrochemical events in photosystems of plant cells. Derivation and application, J. Photochem. Photobiol. B 91 (2008) 58–65.
[43] W.J. Vredenberg, Analysis of initial chlorophyll fuorescence induction kinetics in chloroplasts in terms of rate constants of donor side quenching release and electron trapping in photosystem II, Photosynth. Res. 96 (2008) 83–97.
[44] J.J.S. van Rensen, W.J. Vredenberg, Higher concentration of QB-nonreducing photosystem II centers in triazine-resistant Chenopodium album plants as revealed by chlorophyll fluorescence studies, J. Plant Physiol. (2009), doi:10.1016/j.plph.2009.04.011.
[45] G.H. Krause, P. Jahns, Non-photochemical energy dissipation determined by chlorophyll fluorescence quenching: characterization and function, in: G. Papageorgiou, Govindjee (Eds.), Chlorophyll a Fluorescence: A Signature of Photosynthesis, Advances in Photosynthesis and Respiration, Vol. 19, Springer, Dordrecht, the Netherlands, 2004, pp. 463–495.
[46] R.J. Strasser, M. Tsimilli-Michael, A. Srivastava, Analysis of the fluorescence transient, in: G.C. Papageorgiou, Govindjee (Eds.), Chlorophyll a Fluorescence: A Signature of Photosynthesis. Advances in Photosynthesis and Respiration, Vol. 19, Springer, Dordrecht, 2004, pp. 321–362.
[47] P. Tomek, P. Ilik, D Lazar, M. Stroch, J. Naus, On the determination of QB-nonreducing photosystem II centers from chlorophyll a fluorescence induction, Pl. Science 164 (2003) 665–670.
[48] W.J. Vredenberg, A.A. Bulychev, Photo-electrochemical control of photosystem II chlorophyll fluorescence *in vivo*, Bioelectrochem. 57 (2002) 123–128.
[49] U. Schreiber, Pulse-amplitude modulation (PAM) fluorometry and saturation pulse method: an overview, in: G. Papageorgiou, Govindjee (Eds.), Chlorophyll a Fluorescence: A Signature of Photosynthesis, Springer, Dordrecht, the Netherlands, 2004, pp. 279–319.
[50] K. Maxwell, G.N. Johnson, Chlorophyll fluorescence—a practical guide, J. Exp. Bot. 51 (2000) 659–668.
[51] W.F.J. Vermaas, G. Renger, G. Dohnt, The reduction of the oxygen-evolving system in chloroplasts by thylakoid components, Biochim. Biophys. Acta 764 (1984) 194–202.
[52] H.H. Robinson, A.R. Crofts, Kinetics of the oxidation reduction reactions of the photosystem II quinone acceptor complex and the path for deactivation, FEBS Lett. 151 (1983) 221–226.
[53] B.A. Diner, Dependence of the deactivation reactions of Photosystem II on the redox state of plastoquinone pool A varied under anaerobic conditions; equilibria on the acceptor side of Photosystem II, Biochim. Biophys. Acta 460 (1977) 247–258.
[54] S. Boisvert, D. Joly, R. Carpentier, Quantitative analysis of the experimental O-J-I-P chlorophyll induction kinetics. Apparent activation energy and origin of each kinetic step, FEBS Lett. 273 (2006) 4770–4777.
[55] N.R. Baker, Chlorophyll fluorescence: a probe of photosynthesis in vivo, Annu. Rev. Plant Biol. 59 (2008) 89–113.
[56] D.M. Kramer, G. Johnson, O. Kiirats, G.E. Edwards, New fluorescence parameters for determination of QA redox state and excitation energy fluxes, Photosynth. Res. 79 (2004) 209–218.
[57] S.M. Walas, Modeling with Differential Equations in Chemical Engineering, Butterworth-Heinemann, Boston, 1991.